ELSEVIER

Polymer 42 (2001) 7449–7454

polymer

www.elsevier.nl/locate/polymer

Morphological study of conductive polyaniline/polyimide blends. I. Determination of compatibility by small-angle X-ray scattering method

Moon Gyu Han, Seung Soon Im*

Department of Fiber and Polymer Engineering, Center for Advanced Functional Polymers, Hanyang University, Seoul 133-791, South Korea

Received 23 October 2000; received in revised form 23 January 2001; accepted 9 February 2001

Abstract

Small-angle X-ray scattering patterns of polyaniline (PANI) complexes/polyimide (PI) blends were observed in order to analyze the compatibility between two components of the blends. From the experimental results, it was concluded that the microphase separation or molecular level mixing, which was the reflection of compatibility, was dependent on the kinds of dopant (camphorsulfonic acid (CSA) and dodecylbenzene sulfonic acid (DBSA)), PANI content and the imidization state. On account of self-assembling nature of PANI–DBSA, PANI–DBSA/poly(amic acid) (PAA) shows phase-separated morphology. On the other hand, PANI–CSA/PAA blends exhibited well-mixed and high compatible morphology. Thermal curing of these blends brought about the change of blend morphology, which was in correlation with altered chain structure from PAA into PI, and was also a function of PANI content. It was supposed that conversion from PAA to PI by thermal curing processes led to enhancement of compatibility probably due to higher interaction between two components.

Keywords: Polyaniline/polyimide blends; Morphology; Compatibility

1. Introduction

Polyaniline (PANI) and its derivatives, one of the most promising conducting polymers, were inherently brittle and poor in processability [1,2]. Efforts to improve the mechanical properties and processability, therefore, have been directed to substitute long alkyl chain, etc. on the aromatic ring or nitrogen atom of PANI, copolymerize with other polymer and prepare colloidal dispersed particle, etc. [3–6]. In addition, preparation of conducting polymer blend with another polymer is one of the promising methods to broaden the range of industrial applications [7–11].

After the development by Cao et al. [12], the solution blending method using counterion-induced processability of PANI with functionalized protonic acids like camphorsulfonic acid (CSA) and dodecylbenzene sulfonic acid (DBSA), etc. enabled many kinds of conducting polymer blends with different combinations of dopant anions and co-soluble bulk polymers in the conducting salt form. However, relatively little has been known about the interactions of PANI with other polymers and the role of the counter-anion in the conducting blends. These interactions would determine the phase separation behavior as well as the resulting morphology [13]. The latter will then determine the electrical and mechanical properties of the materials. It is also well known in polymer science that the morphology and/or the phase distribution are important to understand the relationship between structures and properties as well as to predict properties or even to design new materials with specific characteristics.

In our previous works, electrical and structural property of PANI complexes (PANI–CSA and PANI–DBSA)/polyimide (PI) blends were investigated and compared [14–16]. In these blends, the different chain structures as dopants had an effect on the resulting electrical conductivity and physical properties. The blends, therefore, exhibited different surface morphology, compatibility, and doping characteristics. Hence, the need for profound research about the mixing phase determining blend behavior, such as whether the mixing occurs at the level of molecular chains or phase separation occurs, has inspired our observation of compatibility by small-angle X-ray scattering (SAXS) method. Because morphological characteristics originated from dispersion of conducting component into matrix should have a key role in electrical properties of resulting blends, the goal of this paper is to investigate the effect of the counter-ion on the morphology and miscibility of PANI complexes/PI blends including PANI complexes and PI by SAXS method.

* Corresponding author. Tel.: +82-2-2290-0495; fax: +82-2-2297-5859.
E-mail address: imss007@email.hanyang.ac.kr (S.S. Im).

0032-3861/01/$ - see front matter
PII: S0032-3861(01)00244-0

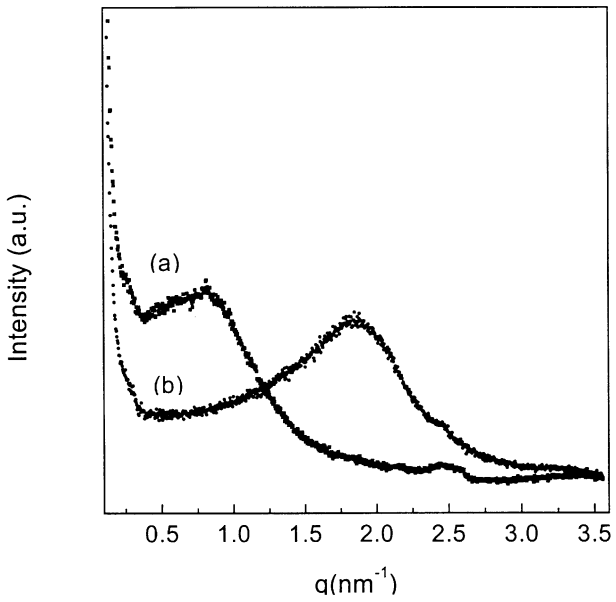

Fig. 1. SAXS patterns for: (a) PANI–CSA, and (b) PANI–DBSA.

2. Experimental

2.1. Chemicals and preparation of samples

Aniline (synthetic grade from Aldrich) was purified by distillation in vacuum before use and ammonium peroxydisulfate ($(NH_4)_2S_2O_8$), HCl and NH_4OH were used as received. CSA (from Aldrich), DBSA (from Kando Chemical) and *N*-methyl-2-pyrrolidinone (NMP, from Aldrich) were also used as received. 4,4′-Oxydianiline (ODA, from TCI) and pyromellitic dianhydride (PMDA, from TCI) for the synthesis of polyamic acid (PAA) were dried and recrystallized.

The PANI–HCl powder was synthesized by the oxidative polymerization of aniline in 1 M aqueous HCl with $(NH_4)_2S_2O_8$ as oxidant, which is similar to the method used by MacDiarmid and co-workers [17]. PANI emeraldine base (EB) was prepared by treating the PANI–HCl powder in 0.1 M NH_4OH solution for 4 h. The PANI complexes (PANI–CSA and PANI–DBSA) solutions and PAA solution was also prepared as described in our previous work [14,15]. These two solutions were mixed, and then stirred at proper ratios for fixed time. PANI complexes/PAA films were prepared by casting these solutions from NMP on the petri dish and drying under dynamic vacuum at 50–60°C. The compositions of the blends were expressed in weight ratios between two components. PANI complexes/PAA films were converted to PANI complexes/PI by thermal imidization. The imidization was proceeded at 120, 150, 180, 210 and 250°C for each 30 min stepwise. Hereafter, PANI–CSA/PI and PANI–DBSA/PI blends with proper weight fraction of PANI will be designated as C and D, respectively. Behind the C and D, the weight percent of PANI are presented. Thermal curing temperature was attached behind the weight fraction indicating number. For example, PANI–CSA/PI blends containing 50 wt% PANI and cured up to 180°C will be nominated as C50180.

2.2. Characterizations

Wide-angle X-ray diffraction (WAXD) and SAXS patterns were obtained by Rigaku model D/Max-2000 equipped with SAXS measuring system. The scattering angle ranges 0.1–3 and 5–40° for SAXS and WAXD measurement, respectively. The X-ray source was 40 kV and 160 mA. The scattered intensity for the SAXS measurements was plotted over the scattering vectors, $q = (4\pi/\lambda)\sin\theta$, where 2θ is the total scattering angle and λ the wave length (Cu Kα radiation, $\lambda = 1.54$ Å) generated from rotating anode source which was monochromatized by crystal monochromator. The scattering curves were collected by a point focusing scintillation detector. All patterns were obtained without any correction or subtraction.

3. Results and discussions

In Fig. 1, SAXS patterns of PANI–CSA and PANI–DBSA are presented for the basic analysis of starting materials. A SAXS peak is shown for PANI–CSA around $2\theta = 1.235°$ ($q = 0.879\ nm^{-1}$), which corresponds to a periodic distance of 64.70 Å. In case of PANI–DBSA, however, intense peak at $2\theta = 2.645°$ ($q = 1.883\ nm^{-1}$) is present, which in turn corresponds to that of 33.36 Å probably attributed to the layered structure resulting from interchain spacing induced by dopant DBSA of which the alkyl side chain acts as spacers between the PANI backbones frequently observed by WAXD patterns [18,19]. It was also reported in our previous paper by WAXD patterns that the PANI–DBSA/PAA blends exhibited layered structure [15]. In this paper, it was reported that different structures of dopants affect both the crystalline structure and long spacing of PANI salts irrespective of using the same solvent for film casting process. Unexpectedly, the periodic distance of PANI–CSA is longer than PANI–DBSA, although PANI–CSA generally has no layered structure like PANI–DBSA. The structure of PANI–CSA prepared from NMP has been known to have little crystalline structure [20]. While, PANI–CSA prepared from *m*-cresol and HFIP solution, etc. has an improved crystalline structure [21,22]. This fact suggests that the crystalline structure of PANI complexes is varied as solvent, i.e. interactions between the polymer and the solvent. In other words, in solution processed PANI, the good solvent such as *m*-cresol would help the polymer chains expand from the initial compact coil conformation. PANI–CSA had some crystalline structure in spite of using NMP as a solvent and the crystalline structure was further improved with annealing in our previous WAXD results [14,15]. Based on these results, the crystalline structure surely exists in PANI–CSA. As the spacing or repetition due to one amorphous and one

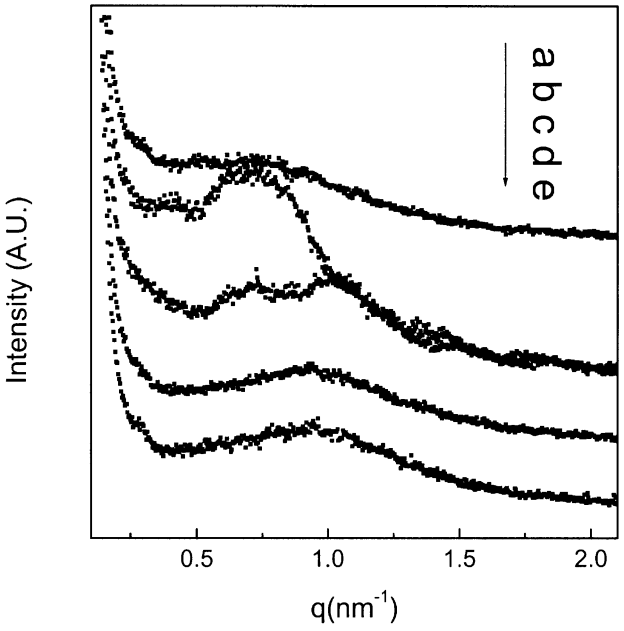

Fig. 2. SAXS patterns for: (a) PAA and its imidized samples up to the respective temperatures, (b) imidized up to 120°C, (c) 150°C, and (d) 180°C.

crystalline layer is generally 5–15 nm from Bragg relation, long period of 64.70 Å of PANI–CSA observed from Fig. 1(a) can also be suggested that the repeating crystallites and amorphous phase coexists in this polymer. Hence, periodic distance, in other words, long spacing, which is longer than layered PANI–DBSA about twice, may be due to this crystalline structure leading to electron density differences.

In Fig. 2, SAXS patterns of PAA are expressed as a function of curing condition up to respective temperatures (non-cured, 120, 150, 180 and 210°C). A peak at $q \approx 0.776\ \mathrm{nm}^{-1}$, which corresponds to a periodic distance of 8.75 nm, is observed for uncured PAA. Because PI made from PMDA–ODA is semicrystalline polymer [23], the peak probably originates from repetition of crystalline and amorphous phases, i.e. two-phase structure. Another possible suggestion is the existence of heterogeneity involving some kinds of superstructure due to molecular aggregation [24]. Anyway, this peak may be due to the inter-particle interference effect between ordered regions or the region with different electron density which may be due to either of ordered regions distributed randomly and densely or of coexisting ordered and less-ordered region. Therefore, there seems to be absence of the wholly randomly coiled amorphous state, which is generally observed in PAA or PI cured at low temperature (under 250°C) [25]. On thermal curing up to 120°C, this peak becomes sharper probably due to change into additional ordered structure from some of amorphous chain or more pronounced electron density difference as a result of excluding solvent NMP preferentially non-hydrogen bonded with PAA from amorphous region. On increasing temperature up to 150°C, the SAXS patterns show two peaks, one existing at $q \approx 0.776\ \mathrm{nm}^{-1}$, which is already presented in PAA, the other new one existing at $q \approx 1.05\ \mathrm{nm}^{-1}$. This new peak might be due to local — such as surface — evaporation of NMP, hence it gives birth to higher packing between adjacent polymer chains, resulting in decreased periodic distance in the higher q region. With further imidization up to 180°C, the peak revealed at lower q disappears and only the peak located at higher q survives resulting from additional evaporation of NMP. In the case of thermal imidization up to 210°C, the position of peak is not changed. This variance of SAXS patterns with thermal curing can be the result of the cyclization of PAA into PI which seems to give rise to become more compact morphology and to enhance molecular packing resulting from evaporation of solvent NMP hydrogen bonded with PI in the crystalline or amorphous region together with additional change of amorphous chain into crystallites by thermal curing. It was revealed that additional removal of NMP by increasing temperature led to peak shifting toward higher q.

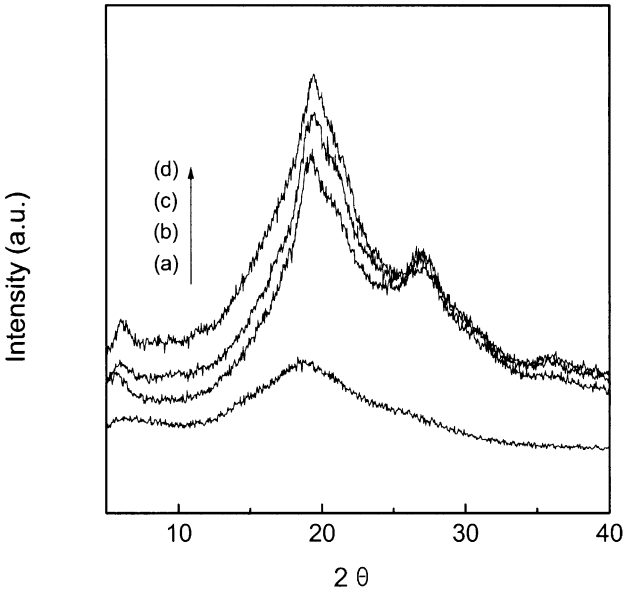

Fig. 3. WAXD patterns for: (a) PAA and its imidized sample up to respective temperatures, (b) imidized up to 120°C, (c) 150°C, and (d) 180°C.

This suggestion was confirmed to be suitable by WAXD measurements as presented in Fig. 3. In PAA condition, the WAXD pattern shows broad peak at $2\theta = 18.7°$ and broad one around $2\theta = 6.1°$, which are generally observed (100) reflection in PAA and (002) reflection frequently observed in the imidized PMDA–ODA, respectively. After thermal curing, the intensity of peaks at $2\theta = 6.1$ and 19.4° are increased and two new peaks at $2\theta = 26.7$ and 35.9° appear. This indicates that the crystallinity is remarkably increased after thermal curing. While, the peak revealed at $2\theta = 18.7°$ shifts to higher angle meaning decreased d-spacing between polymer backbone depending on conversion to be more compact structure. From these results, it should be

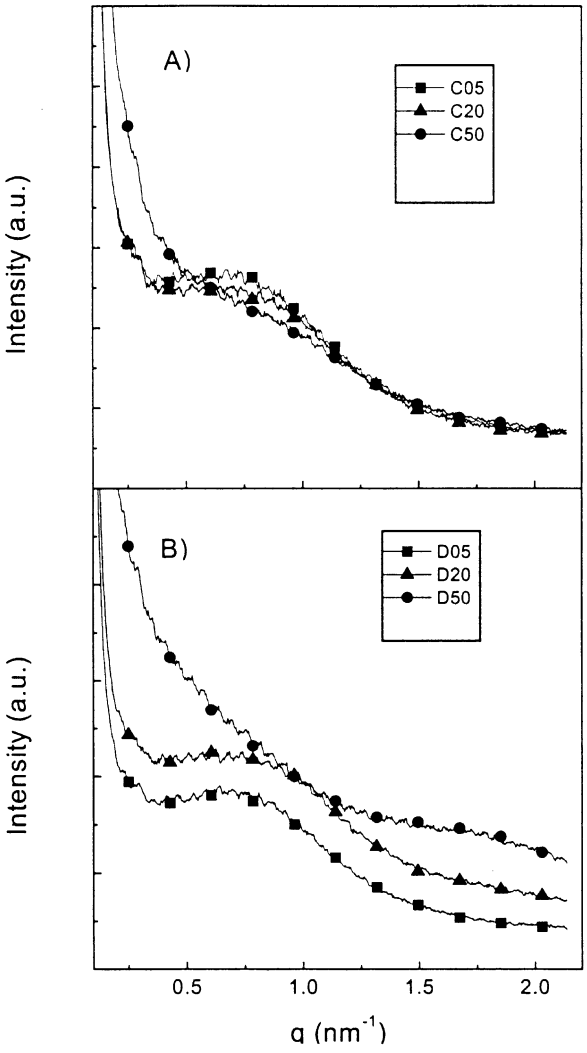

Fig. 4. SAXS patterns for PANI complexes/PAA blends: (A) CSA-doped blends with different PANI content (a) C05, (b) C20 and (c) C50; (B) DBSA-doped blends with different PANI content (a) D05, (b) D20 and (c) D50.

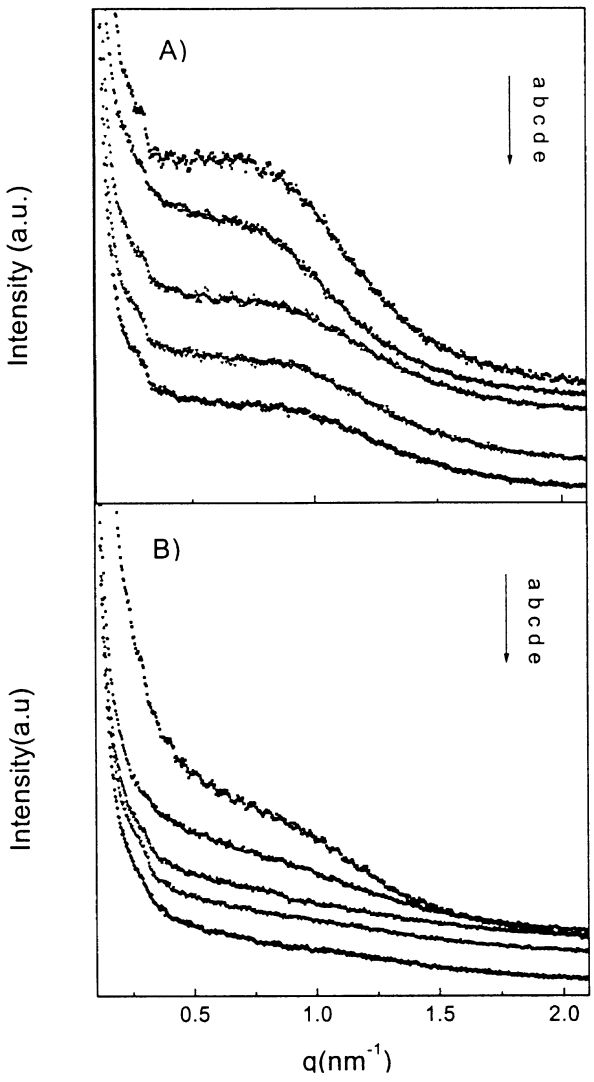

Fig. 5. SAXS patterns of PANI–CSA/PAA blends and their imidized samples up to proper temperatures: (A) 20 wt% blends (a) C20, (b) C20120, (c) C20150, (d) C20180 and (e) C20210; (B) 50 wt% blends (a) C50, (b) C50120, (c) C50150, (d) C50180 and (e) C50210.

concluded that thermal curing of PAA led not only to convert the chain structure to become more compact but also to enhance crystallinity as the evaporation of solvent NMP.

SAXS patterns of PANI–CSA blends as a function of PANI were plotted in Fig. 4(A). In the low PANI content blends (5 and 20 wt%) in Fig. 4(A), SAXS patterns show peak in the peak region of PANI–CSA and PAA (PI). The peak intensity of 20 wt% blend was relatively broadened. The peak of SAXS seems to nearly disappear in case of 50 wt% blend showing only broadened shoulder-like curvature distributed in the peak region of PAA and PANI–CSA. The peak should be maintained if the origin of destruction of respective chain structure is absent. Hence, this disruption of chain structure of both components means molecular level mixing. This distinguished broadening of the peak with the PANI content suggests the high miscibility between two materials. Hopkins et al. [13,26] also reported similar results that crystalline structure of nylon was not disrupted for PANI–CSA/nylon, and they concluded that there was no mixing on a molecular level between two components. They also reported that crystalline-induced phase separation led to crystallization driven formation of conducting polymer blends network with relatively low percolation threshold [27]. In Fig. 4(B), the peak at $q \approx 0.776\ \mathrm{nm}^{-1}$ attributing to PAA is also seen, but the peak at higher q depending on PANI–DBSA is not seen in both 5 and 20 wt% blends. It seems that volume dilution of peak of PAA depending on simple consideration of its weight content is only present. In the case of 50 wt% blend, the peak originating from PAA is shown in the same region with diminished intensity and broadened peak at higher q originating from PANI–DBSA is seen, which means microphase separation between two

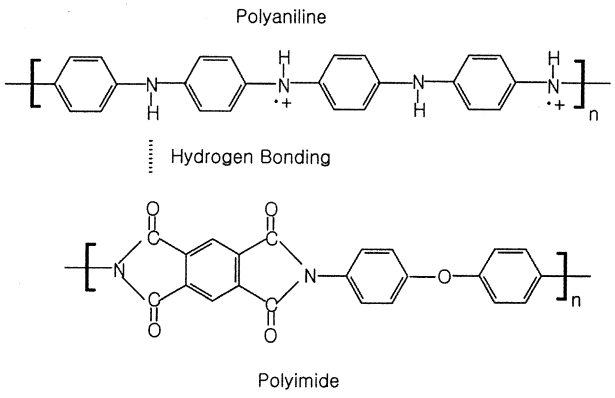

Scheme 1.

components. When the two components were blended, hence, the morphology that is whether microphase separation or molecular level mixing is a function of dopant used. CSA-doped blends seem to have higher miscibility and well-dispersed morphology of molecular mixing than DBSA-doped blends. These results were in good agreement with already reported hypothesis in our previous results supposed from percolation threshold difference by conductivity measurement, T_g analysis by dielectric spectra and thermal response by TGA [15].

SAXS patterns of CSA-doped blends with thermal curing procedure are shown in Fig. 5. In Fig. 5(A), the peak shapes become broaden and shifts toward higher q with increasing temperature. The disappearance of peaks depending on both PANI–CSA and PAA suggests that some kinds of molecular mixing between two components exist, and their driving force might be imidization. Destruction of two-phase morphology with imidization where one phase is crystalline and the other amorphous due to chain mixing may be the result of hydrogen bonding between carbonyl group of PI with amine of PANI without participating in protonation as well as evaporation of solvent. Scheme 1 shows the schematic illustration of possible hydrogen bonding formation in the blends after cyclization of PAA into PI by thermal curing. Although the crystallinity of these blends increase as the thermal curing up to 180°C, this thermal curing results in destruction of SAXS peak. The complete disappearance of peak of a sample cured at higher temperature means that the cross-linking of PANI due to thermal curing might also exist. This phenomenon is more prevalent in case of the 50 wt% blend, in which the peak almost completely disappears with increasing thermal curing temperature. Increased PANI content and thermal curing would promote compatibility between two components probably due to larger hydrogen bonding moiety.

In case of DBSA-doped blends in Fig. 6(A), the peak shifts toward higher q concomitants with broadening as the imidization proceeded, which coincides with the results of PAA as shown in Fig. 2. The existence of characteristic peak of PAA on thermal curing also supports the occurrence of microphase separation. In this sample, distinct disappear-

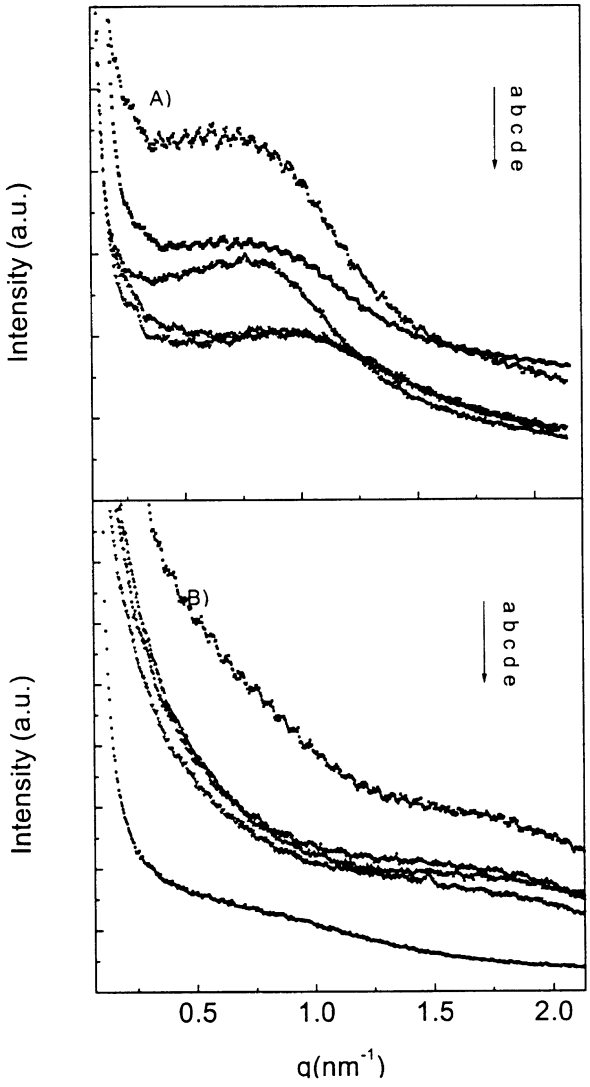

Fig. 6. SAXS patterns of PANI–DBSA/PAA blends and their imidized samples up to proper temperatures: (A) 20 wt% blends (a) D20, (b) D20120, (c) D20150, (d) D20180 and (e) D20210; (B) 50 wt% blends (a) D50, (b) D50120, (c) D50150, (d) D50180 and (e) D50210.

ance of peak depending on thermal cross-linking did not happen, which means higher thermal stability of PANI complex. SAXS patterns of higher PANI content DBSA-doped blends (Fig. 6(B)) contains broadened peak that is related to layered structure of PANI, and it was also additionally broadened after curing. This suggests that the phase-separated layered structure was maintained after thermal curing. But slightly different shape of pattern was obtained in case of imidized up to 210°C. The peak at higher q resulted from PANI–DBSA nearly disappeared, and new broad peak ranging from about 0.5 to 1.25 nm^{-1} appears. This result may be stem from emergence of some new phase obtained by mixing of two components or cross-linking between PANI chains. One fact that may pass over is that PANI also experiences conversion to be more ordered structure under mild thermal annealing [16,28]. These

change of chain structure by thermal treatment and interchain interaction between two components resulting from imidization has an effect on the morphological change.

As mentioned above, the film morphology of the blends would be largely affected by residual NMP content. The intermolecular spacing between adjacent chains of the blends were also decreased with increasing curing step, as in the case of pure PAA (PI). This results in the shifting of the peak to higher angle in SAXS patterns with increasing temperature. The peak shifting occurred in the pure PAA (PI) between 150 and 180°C (Fig. 2). This seemed to appear in similar temperature range in the blends (Figs. 5(A) and 6(A)). The observed NMP content by TGA analysis [15] of the blends at respective curing stage were 12, 4, 1 and 0.2 wt% for DBSA-doped blends and 20, 11, 9 and 4 wt% for CSA-doped blends, respectively, at room temperature, 120, 150, 180 and 210°C. When the curing temperature was 250°C, almost all NMP seemed to be evaporated in both samples. In all curing step, CSA-doped blends contain higher amount of NMP than DBSA-doped blends, which is due to higher molar attraction of CSA with NMP. Hydrophobic natures of long alkyl chain of DBSA expel the access of NMP. Anyway, the additional evaporation of residual NMP in the blends results in the increased compaction of polymer chains, which induced the shifting of SAXS peak to higher temperature.

The results may be summarized as follows: Some kinds of molecular mixing or phase separation were the functions of dopants, blend compositions and imidization temperatures, etc. On thermal treatment, CSA-doped PANI seems to bring about molecular mixing with PI, while DBSA-doped PANI seldom exhibited molecular mixing with PI probably due to phase-separated morphology between two components. In this way, hence, the SAXS measurements enabled tracing morphological variance depending on compatibility between two components of conductive blends. This method would offer a solution to analyze the interaction between conducting polymers with another matrix polymers having crystalline structure.

4. Conclusions

From the experimental results, the following conclusions can be drawn: The compatibility between two components of the PANI/PI could be determined by SAXS patterns. PANI–CSA and PANI–DBSA revealed intrinsically different SAXS patterns exhibiting peak at $2\theta = 1.24$ and 2.65°, respectively. The compatibility was estimated by the level of extinction of characteristic peaks as a result of molecular mixing. In the case of PANI–CSA/PAA blends, this molecular level mixing of two components destructed crystalline structure of both components. The crystalline structure of PANI–DBSA/PAA blends, however, was seldom destructed due to well-defined layered structure of PANI–DBSA. On increasing temperature, PAA was converted into PI with cyclization of backbone accompanying changing into more compacted and crystalline structure. The increase of cyclization into PI ring due to thermal curing led to the higher miscibility with PANI probably because of enhanced interaction between two components such as hydrogen bonding. The lower compatibility of PANI–DBSA/PAA blends, on the contrary to the general prediction, resulted in the reduced percolation threshold of conductivity.

References

[1] Angelopoulos M, Ray A, MacDiarmid AG, Epstein AJ. Synth Met 1987;21:12.
[2] Andreatta A, Cao Y, Chiang JC, Heeger AJ, Smith P. Synth Met 1988;26:383.
[3] Leclerc M, Guay J, Dao LH. Macromolecules 1989;22:641.
[4] Zheng WY, Levon K, Laasko J, Österholm JE. Macromolecules 1994;27:7754.
[5] Pandey SS, Annapoorni S, Malhotra BD. Macromolecules 1993;26:3190.
[6] Armes SP, Aldissi M, Agnew SF, Gottesfeld S. Langmuir 1990;6:1745.
[7] Wessling B, Volk H. Synth Met 1986;15:183.
[8] Ruckenstein E, Park JS. J Appl Polym Sci 1991;42:925.
[9] Bredas J, Dory M, Themans B, Dehalle J, Andre J. Synth Met 1989;28:D533.
[10] Beadle P, Armes SP, Gottesfeld S, Mombourquette C, Houlton R, Andrews WD, Agnew SF. Macromolecules 1992;25:2526.
[11] Chen SA, Fang WG. Macromolecules 1991;24:1242.
[12] Cao Y, Smith P, Heeger AJ. Synth Met 1992;48:91.
[13] Annis BK, Wignall GD, Hopkins AR, Rasmussen PG, Basheer RA. J Polym Sci, Part B: Polym Phys 1997;35:2765.
[14] Han MG, Im SS. J Appl Polym Sci 1998;67:1863.
[15] Han MG, Im SS. J Appl Polym Sci 1999;71:2169.
[16] Han MG, Im SS. Polymer 2000;41:3253.
[17] Wei Y, Jang GW, Hsueh KF, Scherr EM, MacDiarmid AG, Epstein AJ. Polymer 1992;33:314.
[18] Zheng WY, Wang RH, Levon K, Rong ZY, Taka T, Pan W. Macromol Chem Phys 1995;196:2443.
[19] Prosa TJ, Winokur MJ, Moulton J, Smith P, Heeger AJ. Macromolecules 1995;25:436.
[20] Jiang H, Geng Y, Li J, Jing X, Wang F. Synth Met 1997;84:125.
[21] Djurado D, Nicolau YF, Rannou P, Luzny W, Samuelson EJ, Terech P, Bee M, Sauvajol JL. Synth Met 1999;101:764.
[22] Pron A, Rannou P, Gawlitka A, Berner D, Nechtschein M, Kulszweicz-Bajer I, Djurado D. Synth Met 1999;101:729.
[23] Coburn JC, Pottiger MT. Advances in polyimide science and technology. Lancaster, PA: Technomic, 1993. p. 360–74.
[24] Isoda S, Shimada H, Kochi M, Kambe H. J Polym Sci, Polym Phys 1981;19:1293.
[25] Russel TP. J Polym Sci, Polym Phys 1984;22:1105.
[26] Hopkins AR, Rasmussen PG, Basheer RA, Annis BK, Wignall GD. Synth Met 1998;95:179.
[27] Basheer RA, Hopkins AR, Rasmussen PG. Macromolecules 1999;32:4706.
[28] Kobayashi A, Ishikawa H, Amano K, Satoh M, Hasegawa E. J Appl Phys 1993;49:397.